https://doi.org/10.1259/bir.20210466

Received:

Revised: 08 December 2021

Accepted: 15 December 2021 Published online: 07 January 2022

Cite this article as

Ma W, Li J, Chen S, Cai P, Chen S, Chen J, et al. Correlation between contrast-enhanced cone-beam breast computed tomography features and prognostic staging in breast cancer. *Br J Radiol* (2022) 10.1259/bjr.20210466.

# **FULL PAPER**

# Correlation between contrast-enhanced cone-beam breast computed tomography features and prognostic staging in breast cancer

<sup>1</sup>WEI-MEI MA, MS, <sup>2</sup>JIAO LI, MD, <sup>3</sup>SHUANG-GANG CHEN, MS, <sup>2</sup>PEI-QIANG CAI, MD, <sup>2</sup>SHEN CHEN, MS, <sup>2</sup>JIE-TING CHEN, MS, <sup>2</sup>CHUN-YAN ZHOU, MS, <sup>2</sup>NI HE, MD and <sup>2</sup>YAOPAN WU, Professor

<sup>1</sup>Department of Radiology, the Eighth Affiliated Hospital of Sun Yat-sen University, Shenzhen, Guangdong Province, People's Republic of China. China

<sup>2</sup>Department of Medical Imaging, Collaborative Innovation Center for Cancer Medicine, State Key Laboratory of Oncology in South China, Sun Yat-sen University Cancer Center, Guangzhou, Guangdong Province, People's Republic of China, China

<sup>3</sup>Department of Oncology, Yuebei People's Hospital, Shantou University Medical College, Shaoguan, Guangdong Province, People's Republic of China. China

Address correspondence to: Mr Yaopan Wu

E-mail: wuyp@sysucc.org.cn

Ni He

E-mail: *heni@sysucc.org.cn* 

The authors Wei-mei Ma, Jiao Li and Shuang-gang Chen contributed equally to the work. The authors Ni He and Yaopan Wu contributed equally to the work.

**Objective:** To evaluate whether contrast-enhanced cone-beam breast CT (CE-CBBCT) features can risk-stratify prognostic stage in breast cancer.

Methods: Overall, 168 biopsy-proven breast cancer patients were analysed: 115 patients in the training set underwent scanning using v. 1.5 CE-CBBCT between August 2019 and December 2019, whereas 53 patients in the test set underwent scanning using v. 1.0 CE-CBBCT between May 2012 and August 2014. All patients were restaged according to the American Joint Committee on Cancer eighth edition prognostic staging system. Following the combination of CE-CBBCT imaging parameters and clinicopathological factors, predictors that were correlated with stratification of prognostic stage via logistic regression were analysed. Predictive performance was assessed according to the area under the receiver operating characteristic curve (AUC). Goodness-of-fit of the models was assessed using the Hosmer-Lemeshow test.

**Results:** As regards differentiation between prognostic stage (PS) I and II/III, increased tumour-to-breast

volume ratio (TBR), rim enhancement pattern, and the presence of penetrating vessels were significant predictors for PS II/III disease (p < 0.05). The AUCs in the training and test sets were 0.967 [95% confidence interval (CI) 0.938–0.996; p < 0.001] and 0.896 (95% CI, 0.809–0.983; p = 0.001), respectively. Two features were selected in the training set of PS II vs III, including tumour volume [odds ratio (OR)=1.817, p = 0.019] and calcification (OR = 4.600, p = 0.040), achieving an AUC of 0.790 (95% CI, 0.636–0.944, p = 0.001). However, there was no significant difference in the test set of PS II vs III (P > 0.05).

**Conclusion:** CE-CBBCT imaging biomarkers may provide a large amount of anatomical and radiobiological information for the pre-operative distinction of prognostic stage.

**Advances in knowledge:** CE-CBBCT features have distinctive promise for stratification of prognostic stage in breast cancer.

## INTRODUCTION

Breast cancer was the most frequently diagnosed cancer among females and the leading cause of cancer-related death in 2018, globally. Breast cancer is generally recognized as a heterogeneous disease, with a great degree of

diversity in therapeutic response and disease progression, due to different pathological types, immunohistochemical subtypes, histological grade and stages. For example, triplenegative breast cancer (TNBC) is the subtype with the worst prognosis and higher risk of recurrence.<sup>2</sup> Tumour staging

is a crucial step in the treatment process. It provides information on the anatomical extent of disease and enables physicians and patients to predict and compare prognostic outcomes. The most widely used tumour system is the globally recognised tumour, node, metastasis (TNM) staging system established by the American Joint Committee on Cancer (AJCC). It is worth noting that the modified eighth edition introduced a novel prognostic stage (PS) system for breast cancer, with the incorporation of biomarkers (histological grade, oestrogen receptor and progesterone receptor expression, HER2 expression, and multigene panels),<sup>3,4</sup> and the maintenance of the TNM-based anatomic stage (AS) system. Several studies have validated that the discriminatory value of the AJCC eighth edition PS is superior to that of the AS system. 5-9 Lower staging does not indicate the requirement of a lower intensity treatment; it signifies better biological treatment response and clinical outcomes.

Imaging is a vital part of a patient's work-up, not only for diagnosis but also for clinical staging before therapy. Cone-beam breast computed tomography (CBBCT) is a novel imaging tool with high spatial and contrast resolution and making excellent three-dimensional (3D) visualisation of the breast. Noncontrast-enhanced (NCE) CBBCT has superior specificity and sensitivity for breast neoplasms detection and characterisation over mammography, <sup>10</sup> as well as for detecting microcalcification, it also helps with accurate orientation and range measurement of lesions. With the application of additional contrast agents, contrast-enhanced (CE) CBBCT can provide better information about the morphology and haemodynamic features of breast lesions. 11 CE-CBBCT has the advantage of displaying tumour angiogenesis and may help to identify breast cancer immunohistochemical subtypes. 12,13 Previous studies and meta-analyses have indicated that CE-CBBCT is associated with improved diagnostic performance and sensitivity compared to mammography, ultrasonography, and NCE-CBBCT and that its diagnostic accuracy is comparable to that of MRI. 14-16

To the best of our knowledge, thus far, no study has focused on the correlation of CE-CBBCT imaging features with prognoses in breast cancer. Accordingly, we aimed to evaluate the predictive value of CE-CBBCT in such settings.

## **METHODS AND MATERIALS**

This retrospective study was based on data collected from two prospective clinical trial databases approved by the Ethics Committee for the Protection and Privacy of Persons Involved in Clinical Trials (A2011-030-01 and B2019-016-01). All patients provided written informed consent before inclusion in the study. Patients enrolled between August 2019 and December 2019 and between May 2012 and August 2014 were designated to the training (n = 358) and test (n = 212) cohorts, respectively; they underwent CBBCT v. 1.5 and v. 1.0, respectively, at Sun Yat-sen University Cancer Center. The inclusion criteria were as follows: (I) underwent preoperative CE-CBBCT, with the images recorded and saved in the DICOM format; (II) presence of invasive breast cancer, as confirmed by surgical pathology; and (III) availability of complete clinical and surgical pathological information. The exclusion criteria were as follows: (I) receipt

of pre-operative therapy (radiotherapy and neoadjuvant chemotherapy); (II) bilateral breast cancer; (III) presence of ductal carcinoma *in situ*; (IV) history of prosthesis implantation before CBBCT; and (V) poor image quality. In total, 115 patients were enrolled in the training set and 53 in the test set. A flowchart of the patient recruitment process is displayed in Figure 1. All enrolled patients were restaged based on their surgical pathology results according to the eighth edition AJCC PS system.

## CBBCT

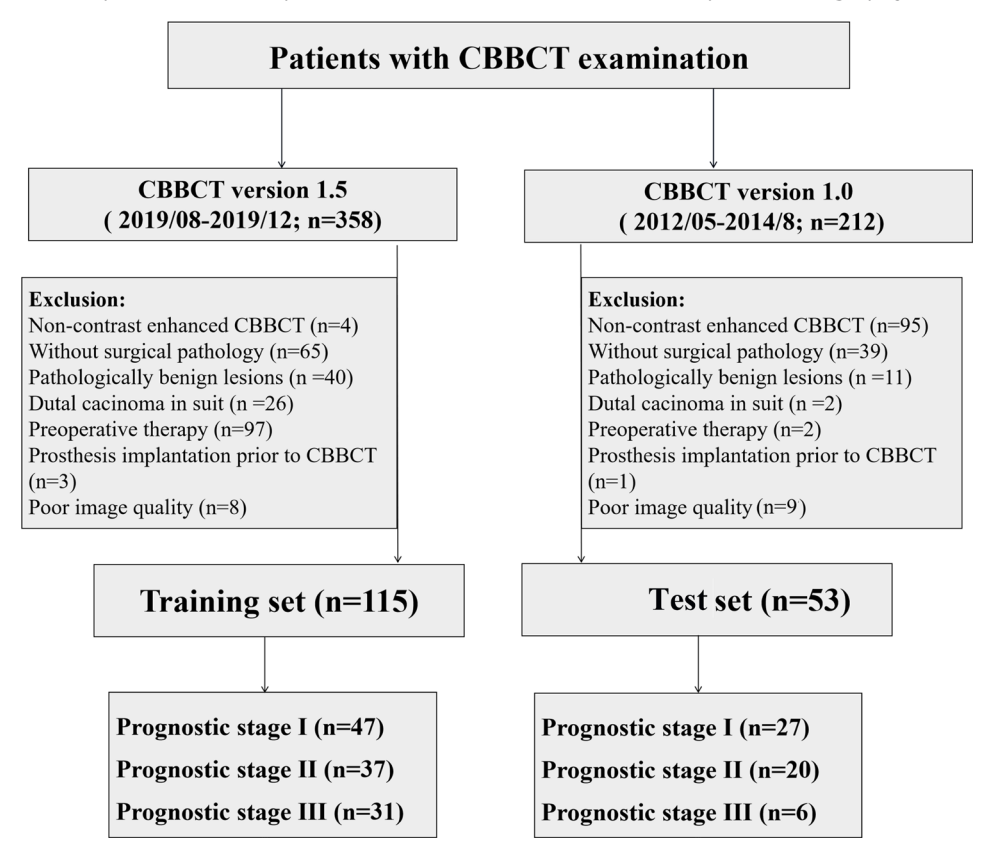
All patients underwent CBBCT (Koning Breast CT, KBCT 1000; Koning Corporation, West Henrietta, NY, USA) of the affected breast located at the centre of rotation with a constant tube exclusively at 49 kVp in a standard manner. <sup>17</sup> A complete CE breast CT scan comprised an initial NCE scan and post-contrast-enhanced scan obtained 50-120s after contrast medium administration. For CE-CBBCT, an intravenous bolus injection of 0.1 mmol/kg Omnipaque (iohexol) (General Electric Medical Systems, USA) was performed at a rate of 2-2.5 ml s<sup>-1</sup> using a power injector, followed by a 30 ml bolus injection of saline solution. Isotropic reconstructions were performed with voxel size of 0.273 mm<sup>3</sup> on each dimension. Specialised 3D visualisation software was utilised to render a 3D model of the breast from the reconstructed images (Visage CS Thin Client/Server, Visage Imaging, v. 7.1, Richmond, USA). v. 1.0 was the first commercialised model of CBBCT system. v. 1.5 is an upgraded system with new product appearance, reduced system footprint, new control software, and image viewer while the specs of the imaging chain and image reconstruction remains the same with v. 1.0. The images acquired from v. 1.0 and v. 1.5 are essentially the same.

## Image analysis

All images were reviewed by a senior resident under the supervision of a breast radiologist with several years of experience; both were blinded to the prior radiological reports and histopathological results. The image parameters extracted from CBBCT included primary tumour size [largest diameter of the tumour, tumour volume, tumour-to-breast volume ratio (TBR) and tumour-to-fibroglandular tissue volume ratio (TFR)], breast density, calcification (absent, present), mass margin (circumscribed, non-circumscribed), contrast enhancement ( $\Delta$ CT), CE patterns of lesions (homogeneous, heterogeneous, rim enhancement), vascular density, penetrating vessels, and tumour-to-nipple distance (TND).

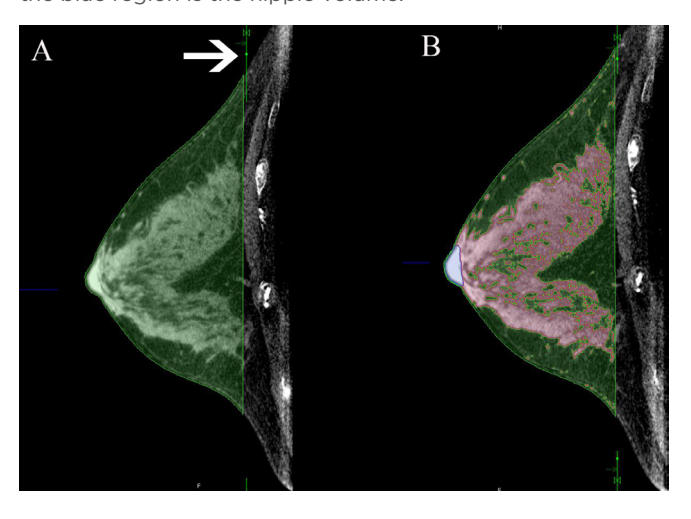
The primary tumour size was measured using CE-CBBCT with 3D threshold segmentation. The breast was delineated from the skin of the breast to the surface of the pectoralis major tangent. The volume of fibroglandular tissue on non-CE images (Figure 2) and tumours on silhouette images (Figure 3) were obtained and calculated by adjusting the threshold. TBR was calculated as the tumour volume/total breast volume  $\times 100$  (%) and TFR as the tumour volume/fibroglandular tissue volume  $\times 100$  (%). Breast density was measured as the volume of fibroglandular tissue/ total breast volume  $\times 100$  (%). Hounsfield units (HUs) was utilised to measure lesion density on CBBCT. As proposed by Prionas et al, contrast enhancement of the breast lesions ( $\Delta$ CT) was standardised to enhancement of fatty tissue and was defined

Figure 1. Flow chart of the patient inclusion process. CBBCT, cone-beam breast computed tomography.



as<sup>11</sup>: ΔCT=ΔCTlesion-ΔCTfat. Homogeneous enhancement was defined as overall diffuse lesion enhancement, heterogeneous enhancement was defined as heterogeneous lesion enhancement. Rim enhancement was defined as the presence of obvious enhancement at the peripheral region of the tumour compared

Figure 2. Schematic diagram of breast density segmentation on the sagittal position of non-contrast enhanced image. The green area outlined by A is the total breast volume at the anterior margin of the pectoralis major tangent (indicated by the white arrow); the red region outlined by B is the fibroglandular volume within the overall range of the above breast; and the blue region is the nipple volume.



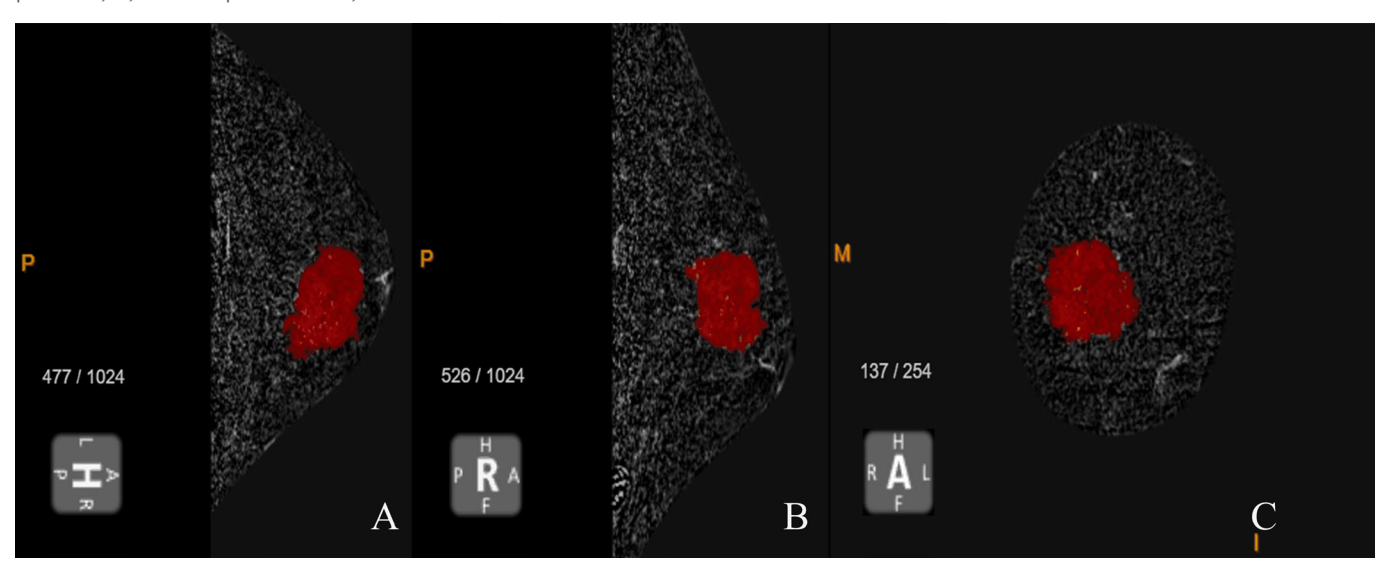
to the centre (Figure 4). The vascular density around the tumour and the presence or absence of penetrating vessels were observed on the 3D silhouette images (Figure 5). TND was measured using 3D images. First, the radiologist selected the two points closest to the nipple and the edge of the mass and then recorded the co-ordinates (x1, y1, z1; x2, y2, z2). Subsequently, 3D TND was calculated as  $0.273*\sqrt{|x1-x2|^2+|y1-y2|^2+|z1-z2|^2}$ . In patients with multiple lesions, only the lesion with the largest diameter was evaluated.

## Statistical analysis

We compared all the parameters across the different PS subgroups using the Kruskal–Wallis test according to normality for continuous variables and Pearson's  $\chi^2$  test or Fisher's exact test for categorical variables.

Multivariable logistic regression analysis using backward elimination with the Wald criterion was performed to screen out independent factors associated with the stratification of prognostic stage in the training set. Next, receiver operating characteristic (ROC) curves were constructed for the determination of the optimal cut-off value for the continuous variables, with the largest Youden index. In addition, multivariate logistic regression analyses were used to further verify the statistically significant predictors in the training set and evaluate the diagnostic performance in the stratification of prognostic stage in the test set. Odds ratios (ORs) and their corresponding 95% confidence intervals (95% CIs), as estimated from logistic regression analysis, were regarded as relative risks. Predictive performance

Figure 3. Segmentation and tumour volume measurement of breast cancer on 3D silhouette imaging. A, axial position; B, sagittal position; C, coronal position. 3D, three-dimensional.



was assessed according to the area under the receiver operating characteristic curve (AUC). Goodness-of-fit of the models was assessed using the Hosmer–Lemeshow (HL) test.

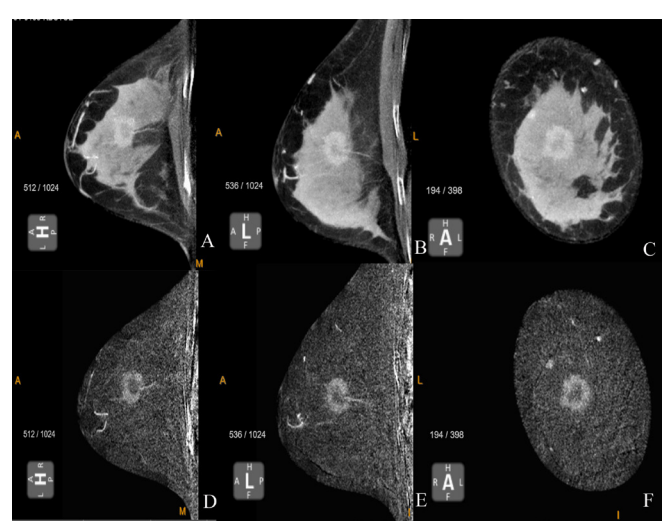
Statistical analyses were performed using SPSS 25.0 statistical package software (SPSS, Chicago, IL) or GraphPad Prism 8.0 software (GraphPad Software Inc., San Diego, CA). Conventional two-sided tests, with a significance level of 0.05, were used in all analyses.

## **RESULTS**

Stage distribution and migration

Patients in both cohorts were restaged according to the AS and PS proposed in the AJCC eighth edition staging manual. The

Figure 4. A 45-year-old female with invasive ductal carcinoma (prognostic stage II). Contrast-enhanced imaging (A-C) and 3D silhouette imaging (D-F) show rim enhancement mass pattern. 3D, three-dimensional; A/D, axial position; B/E, sagittal position; C/F, coronal position.



distribution of the AS and PS stages are presented in Table 1. On using the AS, the percentages of patients with stages I, II, and III disease were 21.7%, 60.9%, and 17.4% in the training set and 37.7%, 43.4%, and 18.9% in the test set, respectively. Employing the PS, the proportions of patients with stages I, II, and III disease were 40.9%, 32.1%, and 27.0% in the training set and 51.0%, 37.7%, and 11.3% in the test set, respectively. In terms of PS, 55 (47.8%) patients in the training set and 24 (45.3%) in the test set underwent stage changing: 31 (training *vs* test: 20.0 *vs* 15.1%) patients were upstaged and 48 (training *vs* test: 27.8 *vs* 30.2%) were downstaged. Migration occurred between Stage I and Stage II/III in 28 patients in the training set (50.9%) and 17 in

Figure 5. (A-C) A 38-year-old female with invasive ductal carcinoma (prognostic stage III). 3D silhouette imaging shows increasing vascular density around the mass. (D-E) A 42-year-old female with invasive ductal carcinoma (prognostic stage II). 3D silhouette imaging shows abnormal vessel penetrating the mass. 3D, three-dimensional; A/D, axial position; B/E, sagittal position; C/F, coronal position.

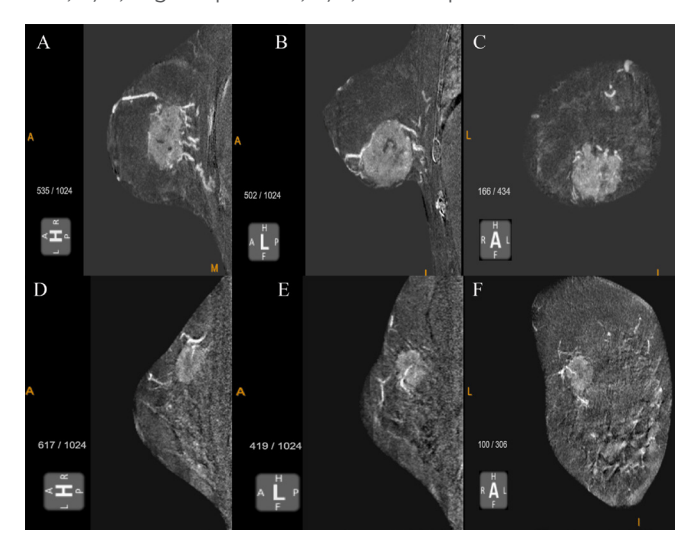


Table 1. Migration of patients from the anatomic to the prognostic system in the training and test sets Percent frequency in the boxes represents the distribution of PSs in the same AS (e.g. among patients in the training set, 88% of patients with anatomic Stage I disease, Stage I status remained, while 12% of patients were upstaged to Stage II with the application of the PS system)

		AJCC eighth PS								
Stage			Training se	et $(n = 115)$	Test set $(n = 53)$					
		I	II	III	N	I	II	III	N	
AJCC eighth AS	I	22 (88)			25	15 (75)			20	
	II	23 (32.8)	27 (38.6)		70	9 (39.1)	11 (47.8)		23	
	III	2 (10)	7 (35)	11 (55)	20	3 (30)	4 (40)	3 (30)	10	
	N	47	37	31	115	27	20	6	53	

AJCC, American Joint Committee on Cancer; AS, anatomic stage; PS, prognostic stage.

Red boxes represent patients with an upstaged prognostic stage, and green boxes those who were downstaged after the application of the PS system. The blue boxes indicate those with an unchanged stage.

the test set (70.8%), which was a relatively frequent change. The most striking change was the significantly increased proportion of PS I disease, due to the migration from AS II and III to PS I. Detailed information on the stage migration that occurred when switching from the AS to PS is shown in Table 1. All the patients in the test set were followed-up; four patients (7.54%) had disease recurrence during the median follow-up of 47.4 months (ranging from 25.8 to 69.0 months) and exhibited clinically confirmed distant metastasis. Two of these patients had PS III and two had PS II disease. The remaining 49 patients (92.46%) did not show disease recurrence after the median follow-up period of 66.94 months (ranging from 14.8 to 84.6 months).

## PREDICTION OF PROGNOSTIC STAGE

The patients' descriptive imaging and clinical characteristics are provided in Table 2. The tumour type, mass margin, CE pattern, vascular density, penetrating vessels, tumour size (largest diameter of the tumour, tumour volume, TBR and TFR), and TND varied significantly across the three subgroups. In the multivariable logistic regression analysis with backward elimination selection (Table 3), three CBBCT features were selected as significant classifiers of PS II/III and I breast cancers, including TBR (OR = 2.469, p = 0.047), CE pattern (rim: OR = 22.167, p = 0.002), and penetrating vessels (OR = 27.793, p < 0.001). The goodness-of-fit analysis with the HL test resulted in a p-value of 0.814, which indicated that the model fit well. The optimal cut-off value for TBR was 0.985%, with the highest Youden index (specificity and sensitivity of 83.8 and 77.4%, respectively). According to the optimal cut-off value in the training set, 27 patients in the test set (50.9%) were categorised into the low-TBR group while the remaining 26 (49.1%) were assigned to the high-TBR group. We included the above-mentioned significant predictors in the training set to analyse the test set using multivariate analyses. Increased TBR, rim enhancement pattern, and the presence of penetrating vessels were statistically significantly associated with PS II/III disease. We achieved an AUC of 0.967 (95% CI 0.938-0.996; p < 0.001) for the training set and 0.896 for the test set (95% CI, 0.809-0.983; p = 0.001). The corresponding ROC curves are shown in Figure 6. Additionally, two features were selected in the training set of PS III vs II, including tumour volume (OR = 1.817, p = 0.019) and calcification (OR = 4.600, p= 0.040), achieving an AUC value of 0.809 (95% CI, 0.748-0.871,

p = 0.001). The p-value on the HL test for goodness-of-fit was 0.399. The optimal cut-off point for TV was  $4.78 \, \mathrm{cm}^3$ , with the highest Youden index (specificity and sensitivity of 64.7 and 79.6%, respectively). However, statistical significance was not noted in the test set of PS III vs II (P > 0.05), achieving an AUC of 0.686 (95% CI, 0.492–0.880, p = 0.068).

#### DISCUSSION

In this era of precision and personalised medicine, the value of a single anatomical staging system is considered limited. 18,19 To the best of our knowledge, this study is the first to correlate CE-CBBCT imaging features with PS in breast cancer. In our study, we found that the most frequently observed change was the transition between stages I and II or III in the training and test sets, including the upgrade of AS I to PS II/III and the demotion of AS II/III to PS I. Regardless of histological grade, the prognostic staging of aggressive TNBC is generally upstaged compared to that on anatomical staging. For example, TNBC patients with stage T1N0M0 (AS IA) and low histological grade were upstaged to PS IIA; therefore, it was found that the lowest stage of TNBC was PS IIA. Thus, we categorised patients with PS II and III disease into the high prognostic risk group and those with PS I disease into the low prognostic risk group.

Exact pre-therapeutic tumour sizing plays a key role in determining the type and extent of subsequent surgical and oncological management. Some studies have hypothesised that tumour size is also an important factor in the prediction of receptor status and prognoses. Larger size is related to poor prognoses and more commonly observed in TNBC than in other subtypes.<sup>20</sup> However, compared to conventional twodimensional diameter measurement, 3D tumour volume may be a more appropriate indicator of tumour burden and a better prognosticator for breast cancer patients.<sup>21</sup> Tumour volume demonstrated good ability in the stratification of PS II and III in the training set (p = 0.019), reflecting the tumour burden. Since breast size and density vary individually across different races, patients with the same tumour size have different breast sizes and densities. Thus, given these individual differences, TBR and TFR were applied in this study, as obtained through the 3D visualisation of CBBCT. Vos et al considered TBR to be

Table 2. CBBCT imaging and clinical characteristics of patients in the training set

Variable Age (y)						
		All patients	PSI  ( $n = 47$ )	PS II $(n = 37)$	PS III $(n = 31)$	P value
	<40	16	7 (14.9%)	5 (13.5%)	4 (12.9%)	0.966
	>40	66	40 (85.1%)	4 (86.5%)	27 (87.1%)	
$BMI (kg/m^2)$		115	22.442 ± 2.303	22.999 ± 2.828	22.455 ± 2.488	0.519
Menopause status	Pre-menopausal	73	34 (72.3%)	20 (54.1%)	19 (61.3%)	0.215
	Post-menopausal	42	13 (27.7%)	17 (45.9%)	12 (38.7%)	
Side	Left	50	21 (44.7%)	13 (35.1%)	16 (51.6%)	0.385
	Right	65	26 (55.3%)	24 (64.9%)	15 (48.4%)	
Calcification	Absent	29	36 (76.6%)	15 (40.5%)	16 (51.6%)	0.003
	Presence	48	11 (23.4%)	22 (59.5%)	15 (48.3%)	
Mass margin	Circumscribed	22	12 (36.2%)	2 (5.4%)	3 (3%)	0.001
	Non-circumscribed	93	30 (63.8%)	35 (94.6%)	28 (90.3%)	
CE pattern	Homogeneous enhancement	29	26 (55.3%)	6 (16.2%)	0 (0.0%)	<0.001
	Heterogeneous enhancement	41	18 (27.0%)	10 (27.0%)	3 (9.7%)	
	Rim enhancement	45	3 (6.4%)	21 (56.8%)	28 (90.3%)	
Vascular density	Normal	33	24 (51.1%)	3 (8.1%)	6 (19.4%)	<0.001
	Increasing	82	23 (48.9%)	34 (91.9%)	25 (80.6%)	
Penetrating vessels	Absent	47	39 (83.0%)	5 (13.5%)	3 (9.7%)	<0.001
	Presence	89	8 (17.0%)	32 (86.5%)	28 (90.3%)	
Breast density (%)*		115	$35.178 \pm 19.078$	$31.207 \pm 20.337$	$38.733 \pm 18.505$	0.128
∆CT (HU)*		115	$64.008 \pm 36.679$	$54.118 \pm 19.957$	$61.094 \pm 11.805$	0.530
Largest diameter of the tumour (mm)*	mm)*	115	$19.617 \pm 10.229$	$28.784 \pm 13.404$	$33.161 \pm 10.681$	<0.001
Tumour volume (cm³)*		115	$3.070 \pm 3.888$	$4.262 \pm 3.402$	$11.509 \pm 11.906$	<0.001
TBR (%)*		115	$0.607 \pm 0.761$	$1.408 \pm 0.821$	$3.273 \pm 3.266$	<0.001
TFR (%)*		115	$3.375 \pm 3.378$	$6.405 \pm 5.480$	$9.583 \pm 9.284$	<0.001
TND (mm)*		115	$32.426 \pm 13.238$	$22.000 \pm 12.385$	24.807 ± 13.465	0.004

CBBCT, cone-beam breast computed tomography; PS, prognostic stage; BMI, body mass index; CE pattern, contrast-enhanced pattern; HU, Hounsfield unit; ACT, contrast enhancement; TBR, tumour-to-breast volume ratio; TFR, tumour-to-fibroglandular tissue volume ratio; TND, tumour-to-nipple distance; TSD, tumour-to-skin distance.

Qualitative variables are presented as n (%) and quantitative variables as mean ± standard deviation, as appropriate.

6 of 9 birpublications.org/bjr Br J Radiol;95:20210466

Table 3. Multivariate logistic ORs of variables associated with prognostic stage

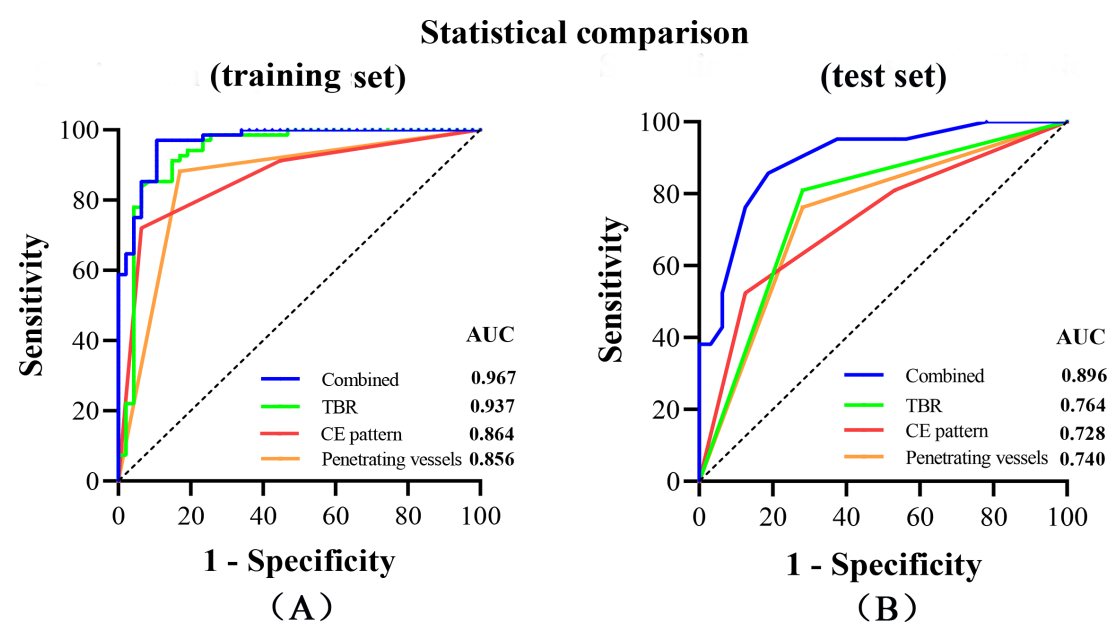
			Training s	et		Cut-off	Test set			
		<i>p</i> -value	OR	95% CI	value	<i>p</i> -value	OR	95% CI		
PS II & III vs	[									
TBR			0.047	2.469	1.010-6.032	≤0.985%	-	1		
						> 0.985%	0.006	12.425	2.042-75.617	
CE pattern		Homogeneous enhancement		1			-	1		
	Heterogeneous enhancement		0.767	1.414	0.255-6.383		0.753	0.725	0.113-4.670	
	Rim enhar	Rim enhancement		22.176	3.115-157.859		0.031	9.551	1.228-74.299	
Penetrating Absent			-	1			-	1		
vessels	Present		< 0.001	27.793	6.213-124.332		0.043	4.893	1.054-22.704	
AUC			0.967 (95% CI, 0.938-0.996)				0.896 (95% CI, 0.809-0.983)			
PS III vs II										
Tumour volume		0.019	1.187	1.029-1.370	≤4.78	-	1			
					> 4.78	0.298	2.795	0.404-19.330		
Calcification Absent		Absent	-	1			-	1		
Present		0.040	4.600	1.074-19.705		0.863	1.181	0.180-7.769		
AUC			0.790 (95% CI, 0.636-0.944)				0.686 (95% CI, 0.492-0.880)			

AUC, area under the receiver operating characteristic curve; CI, confidence interval; OR, odds ratio; PS, prognostic stage; TBR, tumour-to-breast volume ratio; CE pattern, contrast-enhanced pattern.

a precise and independent predictor of cosmetic results after breast-conserving surgery.<sup>22</sup> Wen et al reported that TBR was a risk factor for outcomes in breast cancer patients.<sup>23</sup> Our study indicated that TBR was significant in the classification task for high- and low-risk prognostic staging. This result makes sense

because 3D tumour size measurement may provide more useful discriminatory information than linear tumour size alone. Therefore, the proposed definition of TBR on 3D imaging could reflect the overall structural characteristics of tumours and be a significant indicator of the actual tumour burden. This may

Figure 6. ROC curves predicting prognostic stages II and III vs I in the training set (A) and test set (B). AUC, area under the receiver operating characteristic curve; CE, contrast-enhanced; ROC, receiver operating characteristic; TBR, tumour-to-breast volume ratio.



be related to the infiltrative growth pattern and morphological irregularity of higher stage cancer.

Combining the advantages of mammography and MRI, CE-CBBCT can not only aid in the visualisation of the tumour angiogenesis in lesions but also in the observation of calcification. Tumour angiogenesis refers to the proliferation of the blood vessels that infiltrate tumours, with the potential for tumour growth and metastasis. Therefore, the non-invasive radiological assessment of tumour angiogenesis is helpful in the diagnosis and monitoring of breast cancer patients. The subtracted images obtained by contrast-enhanced examination could reveal the presence of enhancing lesions and vascularity. Uhlig et al reported that contrast enhancement on CBBCT could aid in the discrimination of receptor status and immunohistochemical subtypes in breast cancer<sup>12</sup>; however, there were no significant differences in the degree of contrast enhancement between the different prognostic stages. The rim enhancement pattern could be illuminated by peripheral high angiogenesis and central tumour necrosis.<sup>24</sup> Previous studies have reported that the rim enhancement pattern is associated with higher histological grade, negative ER status, and TNBC.<sup>25-27</sup> It could be used as a predictor of metastatic progression in breast cancer.<sup>28</sup> According to the AJCC eighth edition prognostic staging system, significant changes included the upstaging of patients with TNBC and tumours with a high histological grade that were HER2-negative and either oestrogen or progesterone receptor-positive.<sup>3</sup> The presence of penetrating vessels was considered to promote breast cancer cell proliferation, metastasis, and low survival rates because of the association with the upregulation of the CST1 and AGR2 genes, <sup>29,30</sup> usually observed by superb microvascular imaging. This study also found that high-risk prognostic breast cancer tends to exhibit these vascular characteristics by 3D visualisation of novel CBBCT. Our study observed an unfavourable prognostic factor for breast cancer-calcification-which was significantly related to PS III tumours compared to PS II tumours in the training set. Previous studies have shown that calcification in breast cancer, particularly casting-type calcification, <sup>31,32</sup> is associated with migration

capability, leading to bone metastasis, and HER2-enrichment and serves as an unfavourable prognostic factor. At present, there is no accepted lexicon for microcalcification features on CBBCT images, which may influence the significant findings on the association between calcification characteristics and prognoses.

This study has several limitations. First, it was a retrospective study, and patient selection bias may have existed. Second, we measured tumour size by extracting contrast-enhanced regions on 3D images, which may have resulted in the underestimation or understating of the actual tumour burden. In addition, the total breast was defined as the region in front of the anterior margin of the pectoralis major tangent; this may have led to underestimation of the total breast volume in patients with a strong pectoralis major. Further validation in multiple institutions is needed to confirm the utility of CBBCT imaging biomarkers in clinical practice. This study falls under the category of semantics, radiomics and machine learning approaches could reduce the degree of the inter- or intragroup differences caused by manual interpretation, optimise predictors, and promote the development of precision medicine.

## **CONCLUSIONS**

In conclusion, this study revealed an association between CE-CBBCT features and prognostic stage stratification. CE-CBBCT imaging biomarkers may provide a large amount of anatomical and radiobiological information for prognostic prediction.

# **CONFLICTS OF INTEREST**

The authors declare that they have no conflicts of interest concerning this article.

## **FUNDING**

This work was supported by the National Key Research and Development Program of China (grant number 2017YFC0112605) and Guangdong Medical Science and Technology Research Fund of China (grant number A201805).

## **REFERENCES**

- Bray F, Ferlay J, Soerjomataram I, Siegel RL, Torre LA, Jemal A. Global cancer statistics 2018: globocan estimates of incidence and mortality worldwide for 36 cancers in 185 countries. CA Cancer J Clin November 2018; 68: 394–424. https://doi.org/10.3322/caac. 21492
- Waks AG, Winer EP. Breast cancer treatment: a review. *JAMA* 22, 2019; 321: 288–300. https://doi.org/10.1001/jama.2018.
- Giuliano AE, Connolly JL, Edge SB, Mittendorf EA, Rugo HS, Solin LJ, et al. Breast cancer-major changes in the american joint committee on cancer eighth edition cancer staging manual. CA Cancer J Clin July

- 8, 2017; **67**: 290–303. https://doi.org/10.3322/caac.21393
- Giuliano AE, Edge SB, Hortobagyi GN.
  Eighth edition of the ajcc cancer staging
  manual: breast cancer. *Ann Surg Oncol* 2018;
   25: 1783–85. https://doi.org/10.1245/s10434018-6486-6
- Lee SB, Sohn G, Kim J, Chung IY, Lee JW, Kim HJ, et al. A retrospective prognostic evaluation analysis using the 8th edition of the american joint committee on cancer staging system for breast cancer. *Breast Cancer Res Treat* 2018; 169: 257–66. https:// doi.org/10.1007/s10549-018-4682-5
- Abdel-Rahman O. Validation of the 8th ajcc prognostic staging system for breast cancer

- in a population-based setting. *Breast Cancer Res Treat* 2018; **168**: 269–75. https://doi.org/10.1007/s10549-017-4577-x
- Li X, Zhang Y, Meisel J, Jiang R, Behera M, Peng L. Validation of the newly proposed american joint committee on cancer (ajcc) breast cancer prognostic staging group and proposing a new staging system using the national cancer database. *Breast Cancer Res Treat* 2018; 171: 303–13. https://doi.org/10. 1007/s10549-018-4832-9
- 8. Weiss A, Chavez-MacGregor M,
  Lichtensztajn DY, Yi M, Tadros A,
  Hortobagyi GN, et al. Validation study of the
  american joint committee on cancer eighth
  edition prognostic stage compared with the

- anatomic stage in breast cancer. *JAMA Oncol* 1, 2018; 4: 203–9. https://doi.org/10.1001/jamaoncol.2017.4298
- Wong RX, Wong FY, Lim J, Lian WX, Yap YS. Validation of the ajcc 8th prognostic system for breast cancer in an asian healthcare setting. *Breast* 2018; 40: S0960-9776(18)30076-6: 38–44: https://doi.org/10. 1016/j.breast.2018.04.013
- Zhao B, Zhang X, Cai W, Conover D, Ning R. Cone beam breast ct with multiplanar and three dimensional visualization in differentiating breast masses compared with mammography. Eur J Radiol 2015; 84: S0720-048X(14)00290-3: 48–53: https://doi.org/10. 1016/j.ejrad.2014.05.032
- Prionas ND, Lindfors KK, Ray S, Huang S-Y, Beckett LA, Monsky WL, et al. Contrastenhanced dedicated breast ct: initial clinical experience. *Radiology* 2010; 256: 714–23. https://doi.org/10.1148/radiol.10092311
- Uhlig J, Fischer U, von Fintel E, Stahnke V, Perske C, Lotz J, et al. Contrast enhancement on cone-beam breast-ct for discrimination of breast cancer immunohistochemical subtypes. *Transl Oncol* 2017; 10: S1936-5233(17)30295-4: 904–10: https://doi.org/ 10.1016/j.tranon.2017.08.010
- Ma Y, Liu A, O'Connell AM, Zhu Y, Li
  H, Han P, et al. Contrast-enhanced cone
  beam breast ct features of breast cancers:
  correlation with immunohistochemical
  receptors and molecular subtypes. *Eur Radiol*2021; 31: 2580–89. https://doi.org/10.1007/
  s00330-020-07277-8
- 14. He N, Wu Y-P, Kong Y, Lv N, Huang Z-M, Li S, et al. The utility of breast cone-beam computed tomography, ultrasound, and digital mammography for detecting malignant breast tumors: a prospective study with 212 patients. Eur J Radiol 2016; 85: S0720-048X(15)30172-8: 392-403: https:// doi.org/10.1016/j.ejrad.2015.11.029
- Wienbeck S, Fischer U, Luftner-Nagel S, Lotz J, Uhlig J. Contrast-enhanced cone-beam breast-ct (cbbct): clinical performance compared to mammography and mri. Eur Radiol September 2018; 28: 3731–41. https://doi.org/10.1007/s00330-018-5376-4
- Uhlig J, Uhlig A, Biggemann L, Fischer U, Lotz J, Wienbeck S. Diagnostic accuracy of cone-beam breast computed tomography: a systematic review and diagnostic metaanalysis. *Eur Radiol* 2019; 29: 1194–1202. https://doi.org/10.1007/s00330-018-5711-9

- Wienbeck S, Uhlig J, Luftner-Nagel S, Zapf A, Surov A, von Fintel E, et al. The role of cone-beam breast-ct for breast cancer detection relative to breast density. Eur Radiol 2017; 27: 5185–95. https://doi.org/10. 1007/s00330-017-4911-z
- 18. Yi M, Mittendorf EA, Cormier JN, Buchholz TA, Bilimoria K, Sahin AA, et al. Novel staging system for predicting disease-specific survival in patients with breast cancer treated with surgery as the first intervention: time to modify the current american joint committee on cancer staging system. *J Clin Oncol* 10, 2011; 29: 4654–61. https://doi.org/10.1200/JCO.2011.38.3174
- Bagaria SP, Ray PS, Sim M-S, Ye X, Shamonki JM, Cui X, et al. Personalizing breast cancer staging by the inclusion of er, pr, and her2. *JAMA Surg* 2014; 149: 125–29. https://doi. org/10.1001/jamasurg.2013.3181
- Net JM, Whitman GJ, Morris E, Brandt KR, Burnside ES, Giger ML, et al.
   Relationships between human-extracted mri tumor phenotypes of breast cancer and clinical prognostic indicators including receptor status and molecular subtype.
   Curr Probl Diagn Radiol 2019; 48: S0363-0188(18)30157-9: 467-72: https://doi.org/10.1067/j.cpradiol.2018.08.003
- Hwang K-T, Han W, Lee SM, Choi J, Kim J, Rhu J, et al. Prognostic influence of 3-dimensional tumor volume on breast cancer compared to conventional 1-dimensional tumor size. *Ann Surg Treat Res* 2018; 95: 183–91. https://doi.org/10. 4174/astr.2018.95.4.183
- Vos EL, Koning AHJ, Obdeijn I-M, van Verschuer VMT, Verhoef C, van der Spek PJ, et al. Preoperative prediction of cosmetic results in breast conserving surgery. *J Surg Oncol* 2015; 111: 178–84. https://doi.org/10. 1002/jso.23782
- 23. Wen J, Ye F, Huang X, Li S, Yang L, Xiao X, et al. The tumor-to-breast volume ratio (tbr) predicts cancer-specific survival in breast cancer patients who underwent modified radical mastectomy. *Tumour Biol* 2016; 37: 7493–7500. https://doi.org/10.1007/s13277-015-4382-2
- Metz S, Daldrup-Unk HE, Richter T, Räth C, Ebert W, Settles M, et al. Detection and quantification of breast tumor necrosis with mr imaging: value of the necrosis-avid contrast agent gadophrin-3. *Acad Radiol* 2003; 10: 484–90. https://doi.org/10.1016/s1076-6332(03)80056-9

- Dogan BE, Gonzalez-Angulo AM, Gilcrease M, Dryden MJ, Yang WT. Multimodality imaging of triple receptor-negative tumors with mammography, ultrasound, and mri. AJR Am J Roentgenol 2010; 194: 1160–66. https://doi.org/10.2214/AJR.09.2355
- Lee SH, Cho N, Kim SJ, Cha JH, Cho KS, Ko ES, et al. Correlation between high resolution dynamic mr features and prognostic factors in breast cancer. *Korean J Radiol* 2008; 9: 10–18. https://doi.org/10.3348/kjr.2008.9.1.
- 27. Schmitz AMT, Loo CE, Wesseling J, Pijnappel RM, Gilhuijs KGA. Association between rim enhancement of breast cancer on dynamic contrast-enhanced mri and patient outcome: impact of subtype. *Breast Cancer Res Treat* 2014; 148: 541–51. https://doi.org/10.1007/s10549-014-3170-9
- Song SE, Shin SU, Moon HG, Ryu HS, Kim K, Moon WK. MR imaging features associated with distant metastasis-free survival of patients with invasive breast cancer: a case-control study. *Breast Cancer Res Treat* April 2017; 162: 559–69. https://doi.org/10.1007/s10549-017-4143-6
- 29. Dai D-N, Li Y, Chen B, Du Y, Li S-B, Lu S-X, et al. Correction to: elevated expression of cst1 promotes breast cancer progression and predicts a poor prognosis. *J Mol Med (Berl)* 2019; 97: 1213–14. https://doi.org/10.1007/s00109-019-01806-9
- Park AY, Han M-R, Park KH, Kim JS, Son GS, Lee HY, et al. Radiogenomic analysis of breast cancer by using b-mode and vascular us and rna sequencing. *Radiology* April 2020; 295: 24–34. https://doi.org/10.1148/radiol. 2020191368
- Hu Y, Xu W, Zeng H, He Z, Lu X, Zuo D, et al. OXPHOS-dependent metabolic reprogramming prompts metastatic potential of breast cancer cells under osteogenic differentiation. *Br J Cancer* November 2020;
   123: 1644–55. https://doi.org/10.1038/s41416-020-01040-y
- Sharma T, Sharma A, Maheshwari R, Pachori G, Kumari P, Mandal CC. Docosahexaenoic acid (dha) inhibits bone morphogenetic protein-2 (bmp-2) elevated osteoblast potential of metastatic breast cancer (mda-mb-231) cells in mammary microcalcification. *Nutr Cancer* 2020; 72: 873–83. https://doi.org/10.1080/01635581. 2019.1651879